Viscoelastic Relaxation of the Nuclear Envelope Does Not Cause the Collapse of the Spindle After Ablation in *S. pombe*

Parsa Zareiesfandabadi[1, a)] and Mary Williard Elting[1, 2]

[1)]*Department of Physics, North Carolina State University, Raleigh, NC 27695, USA*
[2)]*Cluster on Quantitative and Computational Developmental Biology, North Carolina State University, Raleigh, NC 27695, USA*

[a)]Corresponding author: pzareie@ncsu.edu

Abstract. A large molecular machine called the mitotic spindle is responsible for accurate chromosome segregation in eukaryotic cells. The spindle consists of protein filaments known as microtubules and microtubule-associated proteins such as motors and crosslinkers, which help impart its organization. In the case of the fission yeast *S. pombe*, these form a single bundle inside the nucleus. During spindle elongation, sliding by motor proteins provides an internal source of extensile forces, which are resisted by the compressive forces of the nuclear envelope. To probe the sources of this force balance, we cut the spindle using focused laser light at various stages of spindle elongation. We find that the spindle pole bodies collapse toward each other post-ablation. While this basic behavior has been previously observed, many questions remain about the timing, mechanics, and molecular requirements of this phenomenon. Here, we quantify the time scale of the relaxation and probe its underlying mechanism. We demonstrate that viscoelastic relaxation of the nuclear envelope cannot explain this phenomenon and provide evidence of active forces as the underlying mechanism.

INTRODUCTION

The mitotic spindle machinery is highly conserved across all eukaryotes, likely due to its critical functional role of accurately segregating chromosomes between the two daughter cells, ensuring that both have identical genetic information. The fission yeast *Schizosaccharomyces pombe* is an important model organism used in the study of eukaryotic cell division because it achieves chromosome segregation with a relatively simple spindle that is stereotyped cell to cell and because of its well-developed genetic toolkit. These features make it an ideal model system for the mechanical perturbation of the spindle. *S. pombe* undergoes a closed cell division process [1, 2] - wherein its nuclear envelope remains intact - that can be categorized into four morphologically distinct phases defined by the spindle length and rate of elongation [3]: 1- prophase and spindle formation; 2- metaphase and anaphase A; 3- anaphase B and spindle breakdown. The mitotic spindle (Fig. 1a) is assembled from a single bundle of microtubules [4] and microtubule-associated proteins. The elongation phase of the spindle (phase 3) is mainly driven by sliding apart the interdigitating microtubules at the spindle midzone via motor proteins [4, 5, 6, 7]. This is a crucial step to move the segregated chromosomes as far as possible from each other before the cell itself divides in two.

In the past few decades, laser microsurgery coupled with the use of GFP (green fluorescent protein)-based protein markers have been developed as a powerful technique to observe the mechanical response to a controlled intracellular perturbation. This approach allows thorough ablation of cellular structures within a spatial resolution of $\sim$ 500 nm and temporal resolution on the order of seconds with minimal off-target damage to the cell [8]. This technique has previously been used to probe force balance in the *S. pombe* spindle, and it was observed that ablation was followed by the collapse of the spindle [9, 10]. This previous work hypothesized that extensile forces within the spindle resist compressive forces of nuclear envelope and DNA, leading to the collapse of the spindle after spindle ablation. Here, we probe this hypothesis by measuring the shape change of the nucleus following ablation. Surprisingly, we find that the nuclear envelope's viscoelastic relaxation fails to account for the spindle collapse. Instead, the change of nuclear shape that we observe suggests active pulling from inside the nucleus.

MATERIALS AND METHODS

Schizosaccharomyces pombe strains used in this study are PZ2: h+ GFP-atb2:kanMX ade6- leu1-32 ura4-D18 and PZ20: h+ nmt41-GFP-atb2:hpnMX6 + cut11-meGFP:kanMX6. The sources of PZ2 and PZ20 are Chang Lab stock FC2861 and a gift of Caroline Laplante, respectively. For growth conditions and media preparations, we adapted previously described methods [11]. For imaging, we inoculated cultures from YE5S agar plates into YE5S media and grew at 25 °C for 12-24 hours before imaging. For PZ20, we then washed three times with EMM5S and further grew for 6-18 hours in EMM5S liquid media before imaging.

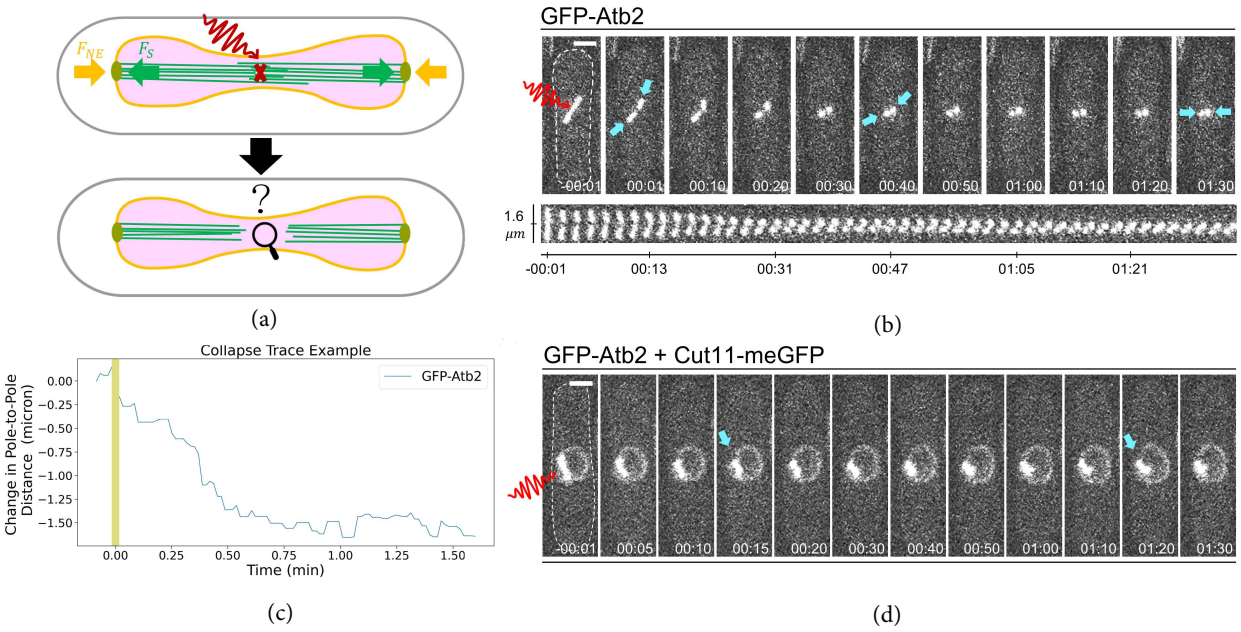

FIGURE 1. The response of the mitotic spindle to laser ablation and its effect on the nuclear envelope. (a) Experimental schematic. To cut the spindle, we target the spindle microtubules (green) in a nucleus (magenta) for laser ablation (red X) and track the response of the spindle, the nuclear envelope (orange), and the spindle pole bodies (lime). Arrows indicate the presumed compressive force of the nuclear envelope oppose by the extensile force of spindle elongation. (b) Example ablation of spindle expressing GFP-Atb2 (alpha-tubulin) during phase two of mitosis. Spindle ends (cyan arrows) collapse toward each other after ablation. Top, highlighted frames; below, a montage of the spindle following ablation. (c) Change in the pole-to-pole distance overtime for the example in (b). (d) Example ablation of spindle expressing GFP-Atb2 and Cut11-meGFP ablated near the midzone during phase two of mitosis. Cyan arrows mark the dents appearing at the nuclear envelope and cytoplasm boundary, indicating inward pulling forces after ablation. (b) and (d) Dashed lines in the first frames indicate the cell boundary. Scale bars, 2 μm. Timestamps, min:sec. We are unable to image during ablation, and the yellow shaded region in (c) indicates this period.

We prepared imaging slides by using a gelatin or agar pad on a microscope glass slide as previously described [12]. We then centrifuged 1 mL of culture at log phase (verified by measuring optical density) at 3000 RCF using a table-top centrifuge, decanted the supernatant, and resuspended the pellet in 20 μL of media. We placed 5 μL of resuspended culture on the pad, covered with a coverslip, and sealed with VALAP (1:1:1 Vaseline:lanolin:paraffin).

We performed all imaging at 22 °C on a Nikon Ti-E stand equipped with an Andor Dragonfly spinning disk confocal fluorescence microscope for GFP imaging and an Andor Micropoint with galvo-controlled steering to deliver 10-15 ns pulses at 20 Hz using a 551 nm dye laser as previously described [13, 14].

We performed image analysis using ImageJ to crop and adjust brightness and contrast in all images. We also used ImageJ to convert the cropped .tif files to .avi for further analysis. We used linear adjustment for brightness and contrast and did not use interpolation or compression at any stage. After the initial cropping and adjustment with ImageJ, we performed all further analyses using home-built Python codes using the Jupyter notebook environment (available upon request). Our software loads in the cropped image stacks as .avi files, records the locations of the distal (presumed spindle pole body) ends of the spindles by manual tracking, and calculates the end-to-end Cartesian distance over time between these two tracked ends.

RESULTS AND DISCUSSION

To investigate the origin of force balance of the mitotic spindle, we ablated the elongating spindles of live *S. pombe* in $n = 73$ cells expressing GFP-Atb2 (alpha-tubulin) on three different dates and $n = 89$ cells expressing GFP-Atb2 plus Cut11-meGFP on five different dates (Fig. 1a). As previously described [9, 10], cutting the spindle causes the fragments to rapidly collapse towards each other (Fig. 1b). We quantified the dynamics of collapse by tracking the

ends of the spindle fragments after ablation and calculated the change in distance between the ends over time. An example of the change in pole-to-pole distance over time is shown in Fig. 1c where a sharp decrease in distance between the poles is evident.

While previous work [9, 10] hypothesized this behavior as passive relaxation of the nuclear envelope or other materials inside of the nucleus (such as chromosomal DNA), its driving force is not yet clear. To test whether nuclear envelope relaxation drives the collapse of the spindle after ablation, we ablated cells expressing GFP-Atb2 and Cut11-meGFP (which localizes to the nuclear envelope) to observe their simultaneous response (Fig. 1d). As shown by arrows in Fig. 1d, during the collapse, the spindle fragments pull the nuclear envelope inward with them, creating local dents at the boundary between the nuclear membrane and the cytoplasm. Such changes in the membrane morphology are inconsistent with the collapse of the spindle driven by the relaxation of tension in the nuclear membrane. This result suggests that active pulling forces internal to the spindle, such as molecular motor proteins, may be at play here (Fig. 1d), and that the surface tension of the nuclear envelope does not cause the collapse.

Work here demonstrates the power of laser ablation as a tool for investigating the mechanics of cytoskeletal machinery. While previous work suggested the presence of compressive forces from outside the spindle, the current work instead suggests that collapse requires pulling from inside the spindle. However, this does not exclude the possibility of additional viscoelastic contributions from the nuclear envelope or chromosomal DNA. Furthermore, the current work raises new questions regarding the origin of the spindle's force balance. To fully explain the spindle's mechanical equilibrium, it will be important to determine the dependence of collapse on spindle-based forces, and the molecular requirements for this force generation.

ACKNOWLEDGMENTS

We thank Caroline Laplante and Fred Chang for providing strains and Kimberly Bellingham-Johnstun, along with the Elting lab members, for helpful discussions. PZ acknowledges the funding support by the Provost's Professional Experience Program, the Office of Undergraduate Research at North Carolina State University, and the National Society of Physics Students. MWE acknowledges support by NIH 1R35GM138083 and NSF 1935260.

REFERENCES

1. J. M. Mitchison, "Chapter 7 physiological and cytological methods for schizosaccharomyces pombe," in *Methods in Cell Biology*, Vol. 4, edited by D. M. Prescott (Academic Press, 1970) pp. 131–165.
2. I. M. Hagan and J. S. Hyams, J. Cell Sci. **89 (Pt 3)**, 343–357 (1988).
3. K. Nabeshima, T. Nakagawa, A. F. Straight, A. Murray, Y. Chikashige, Y. M. Yamashita, Y. Hiraoka, and M. Yanagida, Molecular Biology of the Cell **9**, 3211–3225 (1998).
4. R. Ding, K. L. McDonald, and J. R. McIntosh, Journal of Cell Biology **120**, 141–151 (1993).
5. K. Tanaka and T. Kanbe, Cell Sci. **80**, 253–268 (1986).
6. H. Masuda, T. Hirano, M. Yanagida, and W. Z. Cande, The Journal of Cell Biology **110**, 417–425 (1990).
7. A. Mallavarapu, K. Sawin, and T. Mitchison, Current Biology **9**, 1423–1428 (1999).
8. A. Khodjakov, R. W. Cole, and C. L. Rieder, Cell Motility and the Cytoskeleton **38**(4), 311-317 (1997)
9. A. Khodjakov, S. La Terra, and F. Chang, Current Biology **14**, 1330–1340 (2004).
10. I. M. Tolić-Nørrelykke, L. Sacconi, G. Thon, and F. S. Pavone, Current Biology **14**, 1181–1186 (2004).
11. S. L. Forsburg and N. Rhind, Yeast (Chichester, England) **23**, 173–183 (2006).
12. J.-Q. Wu, J. R. Kuhn, D. R. Kovar, and T. D. Pollard, Developmental Cell **5**, 723–734 (2003).
13. M. W. Elting, M. Prakash, D. B. Udy, and S. Dumont, Current Biology **27**, 2112–2122.e5 (2017).
14. M. A. Begley, A. L. Solon, E. M. Davis, M. G. Sherrill, R. Ohi, and M. W. Elting, preprint bioRxiv , 2020.05.19.104661 (2020).
15. M. W. Elting, C. L. Hueschen, D. B. Udy, and S. Dumont, Journal of Cell Biology **206**, 245–256 (2014).
16. S. Santaguida and A. Amon, Nature Reviews. Molecular Cell Biology **16**, 473–485 (2015).
17. V. P. Singh and J. L. Gerton, Current Opinion in Cell Biology Differentiation and Disease **37**, 9–17 (2015).